Joint ICI and IBI Cancelation for Underwater Acoustic MIMO-OFDM Systems

Mojtaba Beheshti, Mohammad Javad Omidi and Ali Mohammad Doost-Hoseini
Department of Electrical and Computer Engineering
Isfahan University of Technology
Isfahan, Iran 84156-83111
Email: m.beheshti@ec.iut.ac.ir, {omidi, alimdh}@cc.iut.ac.ir,

***Abstract*— A time-domain equalizer (TEQ) is proposed for MIMO-OFDM transmission in underwater acoustic (UWA) channels that simultaneously exhibit large delay and doppler spreads. The aim of the equalizer is to jointly mitigate the intercarrier interference (ICI) and interblock interference (IBI). In this paper, the well known basis expansion model (BEM) is used to describe the UWA channel. Then, the equalizer is derived based on maximizing the signal-to-interference-plus-noise-ratio (SINR). The performance of the proposed approach is demonstrated by numerical simulations. Also, a previously proposed frequency-domain equalizer (FEQ) for communication over doubly selective radio channels is applied to UWA channel and its performance is compared to that of the proposed TEQ.**

Keywords- Underwater acoustic channel, MIMO-OFDM, basis expansion model, intercarrier interference (ICI), interblock interference (IBI), equalization.

I. Introduction

The past few years have witnessed the transition of underwater acoustic (UWA) communication systems from single-input single-output (SISO) schemes to multiple-input multiple-output (MIMO) schemes to provide both spectral efficiency and reliability. Several approaches have been developed for MIMO-UWA communications, including both single-carrier transmissions [1] and multicarrier transmissions in the form of orthogonal frequency-division multiplexing (OFDM) [2], [3]. OFDM is a promising modulation technique for high bit-rate applications, since it avoids interblock interference (IBI) using a cyclic prefix (CP) and mitigates multipath fading with a simple one-tap equalizer. However, long multipath spread of the UWA channel requires a long CP which significantly reduces the spectral efficiency. On the other hand, a short CP leads to IBI. Another limiting factor for OFDM is intercarrier interference (ICI) that is caused by sever Doppler spread encountered in the UWA channel. Therefore, the simple one-tap equalizer cannot be used for MIMO-OFDM in the challenging UWA environment.

Recently, a number of proposals for mitigating the IBI and ICI in UWA channels have been made. In [4] a multiband OFDM modulation with joint equalization and despreading is proposed. Ref. [5] presents two ICI mitigation methods. In the first method, the ICI coefficients are estimated, and minimum mean-square error (MMSE) equalization is performed. In the second method, detection is based on an adaptive decision-feedback equalizer (DFE). Authors in [6] develop a multiuser based OFDM receiver to address IBI in deep water horizontal channels. In [7] an iterative receiver for channel estimation and ICI cancelation is proposed which continually updates the system model to account for channels with large Doppler spread. However, most existing literature, including the above mentioned works, either consider the impact of a short CP or channel Doppler spread.

This paper focuses on interference cancelation for UWA MIMO-OFDM systems in the presence of both long delay spread and large Doppler spread. The paper contains two main contributions: i) a time-domain equalizer (TEQ) is developed to jointly mitigate the ICI and IBI and ii) a previously proposed frequency-domain equalizer (FEQ) for mobile radio channels [8] is employed for interference cancelation in the UWA MIMO-OFDM communications. The rest of the paper is organized as follows. Section II presents the system model, Section III introduces the interference cancelation approaches and Section IV contains the numerical simulations. Finally, Section V concludes the paper.

Notation: Bold lower (upper) letters denote vectors (matrices). Superscripts $(\cdot)^T$ and $(\cdot)^H$ represent transpose and Hermitian, respectively. diag$\{\mathbf{x}\}$ indicates a diagonal matrix with $\mathbf{x}$ as diagonal. x_n denotes the nth element of vector $\mathbf{x}$. $\mathcal{E}\{\cdot\}$ stands for the expectation and $\otimes$ represents the Kronecker product. $\boldsymbol{\mathcal{F}}$ stands for the unitary fast Fourier transform (FFT) matrix. $\mathbf{I}_m$ represents the $m \times m$ identity matrix and the $m \times p$ all-zero matrix is denoted by $\mathbf{O}_{m\times p}$.

II. System model

A MIMO-OFDM system with N_t transmit and N_r receive transducers is considered as in Fig. 1. Input data is partitioned into parallel data sequences and each sequence is arranged into OFDM blocks of length N. The inverse fast Fourier transform (IFFT) of each data block is taken to obtain the time-domain blocks, and each block is preceded by a CP of length c. Then, the time-domain blocks are transmitted in the UWA channel by independent transducers. At the receiver, the CP is discarded and time- or frequency-domain processing is applied. Assuming $x_k^{(t)}[\mathrm{i}]$ is the quadrature phase-shift keying (QPSK) symbol transmitted on the kth subcarrier of the ith OFDM block at the tth transmit transducer, the time-domain sequence transmitted from the tth transducer can then be

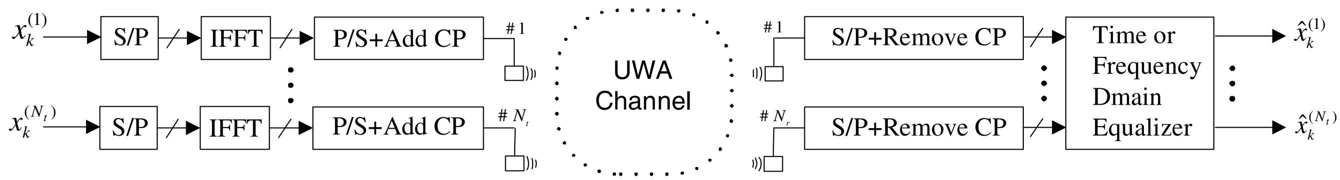

Fig. 1. System model for MIMO-OFDM in UWA channel

written as

$$u^{(t)}[n] = \frac{1}{\sqrt{N}} \sum_{k=0}^{N-1} x_k^{(t)}[i] e^{j2\pi mk/N} \tag{1}$$

where $i = \lfloor n/(N+c) \rfloor$, and $m = n - i(N+c) - c$. The baseband-equivalent description of the received sequence at the rth receive transducer is given by

$$y^{(r)}[n] = \sum_{t=1}^{N_t} \sum_{\theta=0}^{+\infty} g^{(r,t)}[n;\theta] u^{(t)}[n-\theta] + \xi^{(r)}[n] \tag{2}$$

where $g^{(r,t)}[n;\theta]$ is the equivalent baseband impulse response of the link between the tth transmit transducer and the rth receive transducer, and $\xi^{(r)}[n]$ is the additive noise. The noise is assumed to be a zero-mean white complex Gaussian process that is independent of the transmitted sequence.

In this paper, Fourier basis expansion model (BEM) [9] is used to approximate the UWA channel, where the channel is modeled as a time-varying (TV) finite impulse response (FIR) filter $h^{(r,t)}[n;\theta]$, and each tap is expressed as a superposition of complex exponential basis functions. Assuming the channel maximum Doppler spread is bounded by f_{max}, it is possible to accurately model the lth tap of the TV FIR channel $h^{(r,t)}[n;\theta]$ for $n \in \{\, i(N+c)+c+d-L'+1, \ldots, (i+1)(N+c)+d \,\}$ as

$$h^{(r,t)}[n;l] = \sum_{q=-Q/2}^{Q/2} h_{q,l}^{(r,t)}[i] e^{j2\pi qn/K} \tag{3}$$

where d is some synchronization (decision) delay and L' is a constant greater than or equal to the channel order L. The parameter K is the BEM frequency resolution, which is assumed to be an integer multiple of the FFT size, and Q represents the number of TV basis functions satisfying $Q/(2KT) \geq f_{\max}$. The coefficients $h_{q,l}^{(r,t)}[i]$ remain invariant over a period of $(N+L')T$, where T is the sampling time. Substituting the BEM in (2) yields

$$y^{(r)}[n] = \sum_{t=1}^{N_t} \sum_{q=-Q/2}^{Q/2} \sum_{l=0}^{L} e^{j2\pi qn/K} h_{q,l}^{(r,t)}[i] u^{(t)}[n-l] + \xi^{(r)}[n] \tag{4}$$

Using (4) and matrix representation, a block of $N+L'$ samples of the received sequence $y^{(r)}[n]$ can be shown as

$$\mathbf{y}^{(r)}[i] = \sum_{t=1}^{N_t} \Big(\underbrace{\sum_{q=-Q/2}^{Q/2} \mathbf{\Omega}_q[i][\mathbf{O}_1, \mathbf{H}_q^{(r,t)}[i], \mathbf{O}_2](\mathbf{I}_3 \otimes \mathbf{P})(\mathbf{I}_3 \otimes \boldsymbol{\mathcal{F}}^H)}_{\mathbf{G}^{(r,t)}[i]} \times \underbrace{\begin{bmatrix} \mathbf{x}^{(t)}[i-1] \\ \mathbf{x}^{(t)}[i] \\ \mathbf{x}^{(t)}[i+1] \end{bmatrix}}_{\tilde{\mathbf{x}}^{(t)}} \Big) + \boldsymbol{\xi}^{(r)}[i] = \mathbf{G}^{(r)}[i]\tilde{\mathbf{x}} + \boldsymbol{\xi}^{(r)}[i] \tag{5}$$

where i is the block index, $\mathbf{y}^{(r)}[i] = [y^{(r)}[i(N+c)+c+d-L'+1], \ldots, y^{(r)}[(i+1)(N+c)+d]]^T$, $\mathbf{\Omega}_q[i] = \mathrm{diag}\{[e^{j2\pi q(i(N+c)+c+d-L'+1)/K}, \ldots, e^{j2\pi q((i+1)(N+c)+d)/K}]\}$, $\mathbf{O}_1 = \mathbf{0}_{(N+L')\times(N+2c+d-L-L')}$, $\mathbf{O}_2 = \mathbf{0}_{(N+L')\times(N+c-d)}$, $\mathbf{H}_q^{(r,t)}[i]$ is an $(N+L')\times(N+L+L')$ Toeplitz matrix with the first column $[h_{q,L}^{(r,t)}[i], \mathbf{0}_{1\times(N+L'-1)}]$ and the first row $[h_{q,L}^{(r,t)}[i], \ldots, h_{q,0}^{(r,t)}[i], \mathbf{0}_{1\times(N+L'-1)}]$, $\mathbf{x}^{(t)}[i] = [x_0^{(t)}[i], \ldots, x_{N-1}^{(t)}[i]]^T$, $\tilde{\mathbf{x}} = [\tilde{\mathbf{x}}^{(1)T}, \ldots, \tilde{\mathbf{x}}^{(N_t)T}]^T$, $\boldsymbol{\xi}^{(r)}[i] = [\xi^{(r)}[i(N+c)+c+d-L'+1], \ldots, \xi^{(r)}[(i+1)(N+c)+d]]^T$, $\mathbf{G}^{(r)}[i] = [\mathbf{G}^{(r,1)}[i], \ldots, \mathbf{G}^{(r,N_t)}[i]]$ and $\mathbf{P}$ is the CP insertion matrix given by

$$\mathbf{P} = \begin{bmatrix} \mathbf{0}_{c\times(N-c)} & \mathbf{I}_c \\ \mathbf{I}_N & \end{bmatrix}$$

Defining $\mathbf{y}[i] = [\mathbf{y}^{(1)T}[i], \ldots, \mathbf{y}^{(N_r)T}[i]]^T$, $\mathbf{G}[i] = [\mathbf{G}^{(1)T}[i], \ldots, \mathbf{G}^{(N_r)T}[i]]^T$ and $\boldsymbol{\xi}[i] = [\boldsymbol{\xi}^{(1)T}[i], \ldots, \boldsymbol{\xi}^{(N_r)T}[i]]^T$, and using (5), the vector of the received data at all receive transducers is expressed as

$$\mathbf{y}[i] = \mathbf{G}[i]\tilde{\mathbf{x}} + \boldsymbol{\xi}[i] \tag{6}$$

III. Interference Cancelation

In this section, a time-domain as well as a frequency-domain equalizer is proposed for interference cancelation in UWA MIMO-OFDM communication. It is assumed that the UWA channel varies within each OFDM block and the CP length is less than the channel delay spread.

A. Time-domain equalizer

At the receiver, a bank of N_t equalization matrices or filters are applied at each received signal as illustrated in Fig. 2. Then, the outputs of the corresponding filters are summed and passed through the FFT block to recover the transmitted blocks on different transmit paths. Hence, the transmitted block by the ath transmit transducer, $\mathbf{x}^{(a)}[i]$ is estimated as

$$\hat{\mathbf{x}}^{(a)}[i] = \boldsymbol{\mathcal{F}}(\sum_{r=1}^{N_r} \mathbf{G}_e^{(r,a)}[i]\mathbf{y}^{(r)}[i]) \tag{7}$$

Defining $\mathbf{G}_e^{(a)}[i] = [\mathbf{G}_e^{(1,a)}[i], ..., \mathbf{G}_e^{(N_r,a)}[i]]$, (7) is expressed as

$$\hat{\mathbf{x}}^{(a)}[i] = \boldsymbol{\mathcal{F}}\mathbf{G}_e^{(a)}[i]\mathbf{y}[i]. \tag{8}$$

The time-domain equalizer $\mathbf{G}_e^{(a)}[i]$ is designed based on maximizing the SINR at the output of the FFT-demodulator. Substituting the $\mathbf{y}^{(r)}[i]$ from (5) in (7) yields

$$\hat{\mathbf{x}}^{(a)}[i] = \boldsymbol{\mathcal{F}}(\sum_{r=1}^{N_r} \mathbf{G}_e^{(r,a)}[i](\sum_{t=1}^{N_t} \mathbf{G}^{(r,\,t)}[i]\tilde{\mathbf{x}}^{(t)} + \boldsymbol{\xi}^{(r)}[i])) \tag{9}$$

The vector $\tilde{\mathbf{x}}^{(t)}$ in (9) can be written as

$$\tilde{\mathbf{x}}^{(t)} = \mathbf{E}_{-1}\mathbf{x}^{(t)}[i-1] + \mathbf{E}_0\mathbf{x}^{(t)}[i] + \mathbf{E}_1\mathbf{x}^{(t)}[i+1] \tag{10}$$

where $\mathbf{E}_{-1} = [\,\mathbf{I}_N,\ \mathbf{0}_{N\times N},\ \mathbf{0}_{N\times N}\,]^T$, $\mathbf{E}_0 = [\,\mathbf{0}_{N\times N},\ \mathbf{I}_N,\ \mathbf{0}_{N\times N}\,]^T$, and $\mathbf{E}_1 = [\,\mathbf{0}_{N\times N},\ \mathbf{0}_{N\times N},\ \mathbf{I}_N\,]^T$.

Substituting (10) in (9) results in

$$\begin{aligned}\hat{\mathbf{x}}^{(a)}[i] = &\underbrace{\boldsymbol{\mathcal{F}}\sum_{r=1}^{N_r}(\mathbf{G}_e^{(r,a)}[i]\mathbf{G}^{(r,a)}[i])\mathbf{E}_0}_{\mathbf{A}_1}\mathbf{x}^{(a)}[i]\\ &+\underbrace{\boldsymbol{\mathcal{F}}\sum_{r=1}^{N_r}(\mathbf{G}_e^{(r,a)}[i]\mathbf{G}^{(r,a)}[i])\mathbf{E}_{-1}}_{\mathbf{A}_2}\mathbf{x}^{(a)}[i-1]\\ &+\underbrace{\boldsymbol{\mathcal{F}}\sum_{r=1}^{N_r}(\mathbf{G}_e^{(r,a)}[i]\mathbf{G}^{(r,a)}[i])\mathbf{E}_{\,1}}_{\mathbf{A}_3}\mathbf{x}^{(a)}[i+1]\\ &+\underbrace{\boldsymbol{\mathcal{F}}\sum_{r=1}^{N_r}(\mathbf{G}_e^{(r,a)}[i]\sum_{\substack{t=1\\t\neq a}}^{N_t}\mathbf{G}^{(r,\,t)}[i]\tilde{\mathbf{x}}^{(t)})}_{\mathbf{b}_1}+\underbrace{\boldsymbol{\mathcal{F}}(\sum_{r=1}^{N_r}\mathbf{G}_e^{(r,a)}[i]\boldsymbol{\xi}^{(r)}[i])}_{\mathbf{b}_2}\end{aligned} \tag{11}$$

At this point, the kth element of the vector $\hat{\mathbf{x}}^{(a)}[i]$ in (11), which corresponds to the transmitted symbol on the kth subcarrier of the ath transmitted signal, is considered as follows

$$\begin{aligned}\hat{x}_k^{(a)}[i] = &\mathbf{A}_1(k,k)x_k^{(a)}[i] + \sum_{\substack{m=0\\m\neq k}}^{N-1}\mathbf{A}_1(k,m)x_m^{(a)}[i]\\ &+\sum_{m=0}^{N-1}\mathbf{A}_2(k,m)x_m^{(a)}[i-1] + \sum_{m=0}^{N-1}\mathbf{A}_3(k,m)x_m^{(a)}[i+1]\\ &+\mathbf{b}_{1,k} + \sum_{m=0}^{N-1}\boldsymbol{\mathcal{F}}(k,m)\mathbf{b}_{2,m}\end{aligned} \tag{12}$$

where $\mathbf{b}_{\jmath,k}$ is the kth element of vector $\mathbf{b}_\jmath$, $\mathbf{A}_1(k,k)\mathbf{x}_k[i]$ is the desired term and the second term is the ICI component. The third and fourth terms are IBI contributions from the previous and the following blocks, respectively. The fifth term is interference from other transmit transducers or inter-transducer interference (ITI), and the last term is additive noise. The SINR at the kth frequency bin of the ath transmit transducer is defined as

$$\mathrm{SINR}_k^{(a)} = \frac{P_s^{(a,\,k)}}{P_{\mathrm{ICI}}^{(a,\,k)} + P_{\mathrm{IBI}_p}^{(a,\,k)} + P_{\mathrm{IBI}_f}^{(a,\,k)} + P_{\mathrm{ITI}}^{(a,\,k)} + P_{\mathrm{noise}}^{(a,\,k)}} \tag{13}$$

where $P_s^{(a,\,k)}$ represents the signal power and $P_{\mathrm{ICI}}^{(a,\,k)}$ is the ICI power. $P_{\mathrm{IBI}_p}^{(a,\,k)}$ and $P_{\mathrm{IBI}_f}^{(a,\,k)}$ denote the IBI powers due to the previous and the following blocks, respectively. $P_{\mathrm{ITI}}^{(a,\,k)}$ is the interference power caused by other transmit transducers and $P_{\mathrm{noise}}^{(a,\,k)}$ is the noise power. Using (12), the power terms are derived as follows:

$$\begin{aligned}P_s^{(a,k)} &= \sigma_x^2\mathbf{g}_{ek}^{(a)H}[i]\mathbf{g}_k^{(a)}[i]\mathbf{g}_k^{(a)H}[i]\mathbf{g}_{ek}^{(a)}[i],\\ P_{\mathrm{ICI}}^{(a,k)} &= \sigma_x^2\mathbf{g}_{ek}^{(a)H}[i]\mathbf{G}_R^{(a)}[i]\mathbf{E}_0\tilde{\mathbf{I}}_N\mathbf{E}_0^H\mathbf{G}_R^{(a)H}[i]\mathbf{g}_{ek}^{(a)}[i],\\ P_{\mathrm{IBI}_p}^{(a,k)} &= \sigma_x^2\mathbf{g}_{ek}^{(a)H}[i]\mathbf{G}_R^{(a)}[i]\mathbf{E}_{-1}\mathbf{E}_{-1}^H\mathbf{G}_R^{(a)H}[i]\mathbf{g}_{ek}^{(a)}[i]\\ P_{\mathrm{IBI}_f}^{(a,k)} &= \sigma_x^2\mathbf{g}_{ek}^{(a)H}[i]\mathbf{G}_R^{(a)}[i]\mathbf{E}_1\mathbf{E}_1^H\mathbf{G}_R^{(a)H}[i]\mathbf{g}_{ek}^{(a)}[i]\\ P_{\mathrm{ITI}}^{(a,k)} &= \mathbf{g}_{ek}^H[i]\mathbf{R}_{\mathbf{b}}^{(a)}[i]\mathbf{g}_{ek}[i]\\ P_{\mathrm{noise}}^{(a,k)} &= \frac{\sigma_\xi^2}{N}\mathrm{trace}\{\mathbf{G}_e[i]\mathbf{G}_e^H[i]\}\end{aligned} \tag{14}$$

where σ_x^2 and σ_ξ^2 are the QPSK symbol power and the noise variance, respectively, $\mathbf{g}_k^{(r,a)}[i] \triangleq \mathbf{G}^{(r,a)}[i]\mathbf{E}_0\mathbf{e}^{(k)}$, $\mathbf{g}_{ek}^{(r,a)}[i] \triangleq \mathbf{G}_e^{(r,a)H}[i]\boldsymbol{\mathcal{F}}^H\mathbf{e}^{(k)}$, $\mathbf{e}^{(k)}$ is the kth unit vector of size $N\times 1$, $\mathbf{g}_k^{(a)}[i] = [\mathbf{g}_k^{(1,a)T}[i], ..., \mathbf{g}_k^{(N_r,a)T}[i]]^T$, $\mathbf{g}_{ek}^{(a)}[i] = [\mathbf{g}_{ek}^{(1,a)T}[i], ..., \mathbf{g}_{ek}^{(N_r,a)T}[i]]^T$, $\tilde{\mathbf{I}}_N = \mathbf{I}_N - \mathbf{e}^{(k)}\mathbf{e}^{(k)H}$, $\mathbf{G}_R^{(a)}[i] = [\mathbf{G}^{(1,a)T}[i], ..., \mathbf{G}^{(N_r,a)T}[i]]^T$, and $\mathbf{R}_{\mathbf{b}}^{(a)}[i] = \mathcal{E}\{\mathbf{b}\mathbf{b}^H\}$, where $\mathbf{b} = [\sum_{\substack{t=1\\t\neq a}}^{N_t}\tilde{\mathbf{x}}^{(t)T}\mathbf{G}^{(1,\,t)T}[i], ..., \sum_{\substack{t=1\\t\neq a}}^{N_t}\tilde{\mathbf{x}}^{(t)T}\mathbf{G}^{(N_r,\,t)T}[i]]^T$.

Assuming $\mathbf{g}_{ek}^{(a)H}[i]\mathbf{g}_{ek}^{(a)}[i] = 1$ for $0 \le k \le N-1$, and substituting (14) in (13), the SINR at the kth frequency bin of the ath transmit transducer is expressed as

$$\mathrm{SINR}_k^{(a)} = \frac{\mathbf{g}_{ek}^{(a)H}[i]\mathbf{g}_k^{(a)}[i]\mathbf{g}_k^{(a)H}[i]\mathbf{g}_{ek}^{(a)}[i]}{\mathbf{g}_{ek}^{(a)H}[i](\mathcal{R}_k^{(a)}[i] + \frac{\sigma_\xi^2}{\sigma_x^2}\mathbf{I}_{N_r(N+L')})\mathbf{g}_{ek}^{(a)}[i]} \tag{15}$$

where $\mathcal{R}_k^{(a)}[i] = \mathbf{G}_R^{(a)}[i](\mathbf{E}_0(\mathbf{I}_N - \mathbf{e}^{(k)}\mathbf{e}^{(k)T})\mathbf{E}_0^H + \mathbf{E}_{-1}\mathbf{E}_{-1}^H + \mathbf{E}_1\mathbf{E}_1^H)\,\mathbf{G}_R^{(a)H}[i] + \mathbf{R}_{\mathbf{b}}^{(a)}[i]/\sigma_x^2$. The TEQ is derived by solving the following optimization problem:

$$\begin{aligned}&\max_{\mathbf{g}_{ek}^{(a)}[i]}\ \mathbf{g}_{ek}^{(a)H}[i]\mathbf{g}_k^{(a)}[i]\mathbf{g}_k^{(a)H}[i]\mathbf{g}_{ek}^{(a)}[i]\\ &\text{subject to}\ \ \mathbf{g}_{ek}^{(a)H}[i]\left(\mathcal{R}_k^{(a)}[i] + \frac{\sigma_\xi^2}{\sigma_x^2}\mathbf{I}_{N_r(N+L')}\right)\mathbf{g}_{ek}^{(a)}[i] = 1\\ &\text{and}\ \ \mathbf{g}_{ek}^{(a)H}[i]\mathbf{g}_{ek}^{(a)}[i] = 1\end{aligned} \tag{16}$$

The solution of this generalized eigenvalue problem is obtained as [10]

$$\mathbf{g}_{ek,\mathrm{opt}}^{(a)}[i]=\left(\mathbf{G}_{R}^{(a)}[i]\mathbf{G}_{R}^{(a)H}[i]+\frac{\sigma_{\xi}^{2}}{\sigma_{x}^{2}}\mathbf{I}_{N_r(N+L')}+\frac{\mathbf{R}_{\mathbf{b}}^{(a)}[i]}{\sigma_{x}^{2}}\right)^{-1}\times\mathbf{g}_{k}^{(a)}[i] \tag{17}$$

Finally, the optimum equalizer corresponding to the ath transmit transducer is given by

$$\mathbf{G}_{e,opt}^{(a)}[i]=\boldsymbol{\mathcal{F}}^{H}\mathcal{G}_{ek,opt}^{(a)H}[i] \tag{18}$$

where $\mathcal{G}_{ek,opt}^{(a)}[i]=[\mathbf{g}_{e\,0,opt}^{(a)}[i],\ ...,\ \mathbf{g}_{e\,(N-1),opt}^{(a)}[i]]$.

B. Frequency-domain equalizer

In [8] a frequency-domain equalizer (FEQ) was proposed for communication over wireless radio channels. Here, this approach is described and applied to UWA channels. The basic idea behind the FEQ of [8] is that the IBI and ICI affect the received signal in two dimensions i.e, time and frequency dimensions. Therefore, a two dimensional filtering or linear combination can be used to compensate for these interferences. Based on this idea, [8] suggests to estimate the transmitted symbol on the kth subcarrier of the ath transmitted signal as

$$\hat{x}_{k}^{(a)}[i]=\mathbf{v}^{(a,\,k)H}[i](\mathbf{I}_{N_r}\otimes\hat{\mathbf{F}}^{(k)})\mathbf{y}[i] \tag{19}$$

where $\mathbf{v}^{(a,\,k)}$ contains the equalizer coefficients and

$$\hat{\mathbf{F}}^{(k)}=\begin{bmatrix}\mathbf{0}_{1\times L'} & \boldsymbol{\mathcal{F}}^{(k-Q'/2)} & \\ \vdots & \vdots & \\ \mathbf{0}_{1\times L'} & \boldsymbol{\mathcal{F}}^{(k+Q'/2)} & \\ \bar{\mathbf{I}}_{L'} & \mathbf{0}_{L'\times(N-L')} & -\bar{\mathbf{I}}_{L'}\end{bmatrix},$$

where L' and Q' are the equalizer orders in the time and frequency dimensions, respectively, $\boldsymbol{\mathcal{F}}^{(k+q')}$ is the $(k+q')$th row of the FFT matrix $\boldsymbol{\mathcal{F}}$, and $\bar{\mathbf{I}}_{L'}$ is the anti-diagonal identity matrix of size $L'\times L'$.

To design the FEQ $\mathbf{v}^{(a,\,k)}[i]$ for the kth subcarrier of the ath transmit transducer, the following MSE cost function is considered

$$\mathcal{J}[i]=\mathcal{E}\left\{\left|x_{k}^{(a)}[i]-\mathbf{v}^{(a,\,k)H}[i](\mathbf{I}_{N_r}\otimes\hat{\mathbf{F}}^{(k)})\mathbf{y}[i]\right|^{2}\right\} \tag{20}$$

Hence, the minimum MSE (MMSE) coefficients are obtained by solving $\partial\mathcal{J}[i]/\partial\mathbf{v}^{(a,\,k)}[i]=0$ which reduces to

$$\mathbf{v}_{\mathrm{MMSE}}^{(a,\,k)}[i]=\left((\mathbf{I}_{N_r}\otimes\hat{\mathbf{F}}^{(k)})(\mathbf{G}[i]\mathbf{R}_{\tilde{\mathbf{x}}}\mathbf{G}^{H}[i]+\mathbf{R}_{\xi})(\mathbf{I}_{N_r}\otimes\hat{\mathbf{F}}^{(k)H})\right)^{-1}\times(\mathbf{I}_{N_r}\otimes\hat{\mathbf{F}}^{(k)})\mathbf{G}[i]\mathbf{R}_{\tilde{\mathbf{x}}}\bar{\mathbf{e}}^{(k)} \tag{21}$$

where $\mathbf{R}_{\tilde{\mathbf{x}}}=\mathcal{E}\{\tilde{\mathbf{x}}\tilde{\mathbf{x}}^{H}\}=\sigma_{x}^{2}\mathbf{I}_{(3N_tN)}$, $\mathbf{R}_{\xi}=\sigma_{\xi}^{2}\mathbf{I}_{N_r(N+L')}$, and $\bar{\mathbf{e}}^{(k)}$ is the $(3N_tN)\times 1$ unit vector with a 1 in the position $3N(a-1)+N+k$. Fig. 3 depicts the FEQ for the kth subcarrier of the ath transmit transducer.

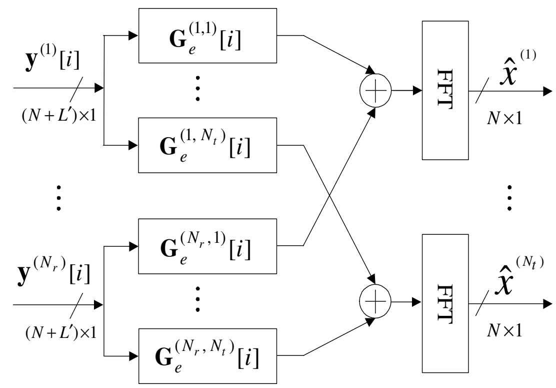

Fig. 2. Proposed time-domain equalizer (Proposed-TEQ)

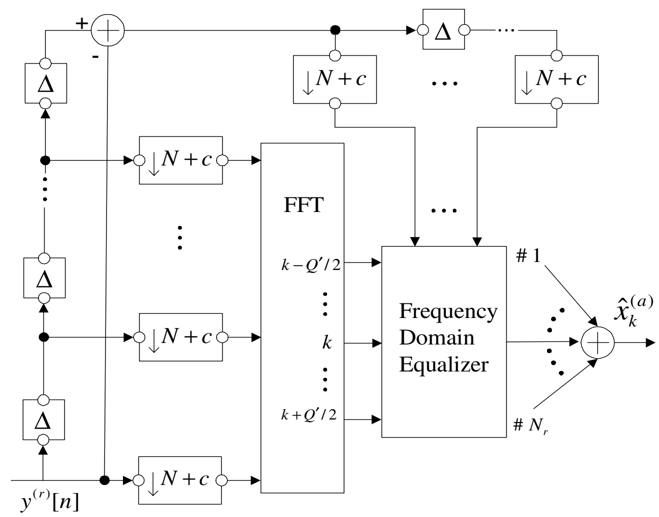

Fig. 3. Proposed frequency-domain equalizer (Proposed-FEQ)

IV. NUMERICAL RESULTS

A single-input multiple-output (SIMO) system with N_r= 2 receive transducers as well as a MIMO system with N_t= 2 transmit and N_r= 4 receive transducers are considered. The simulation parameters are listed below:

- Doppler spread $f_{\max}=50$ Hz
- delay spread $\tau_{\max}=2$ msec
- sampling time $T=100$ μsec
- number of subcarriers $N=128$
- cyclic prefix length $c=14$
- synchronization (decision) delay $d=4$
- discrete Doppler spread $Q/2=2$
- BEM resolution $K=2N$

The UWA channel is simulated as a Rician fading channel [11] with four paths between each transmit and receive transducer pair. To consider a sparse channel, $N_a=4$ nonzero fading coefficients or active taps are spread over L= 20 chip intervals. The active taps are at path delays $\tau_0=0$, $\tau_1=0.4$, $\tau_2=1.1$, and $\tau_3=2$ *msec* and each tap is independently simulated by passing a complex Gaussian random signal with mean $\mu_1+j\mu_2$ and variance

$2\sigma^2_{\mathrm{Rice}}$ through a fading filter [12]. The fading filter has a Gaussian-shaped power spectrum. Moreover, an exponential delay power profile (DPP) is used, i.e. the lth tap power at delay τ_l is $\sigma_l^2 = c_0 \exp(-\tau_l/\tau_{\mathrm{rms}})$, where τ_{rms} is the rms delay spread and c_0 is the normalization constant. The simulated (true) channel is approximated by BEM. Then, the BEM coefficients are obtained by least squares fitting the true channel with the BEM. Also, the Rician factor K_R is defined as $K_R = (\mu_1^2 + \mu_2^2)/(2\sigma^2_{\mathrm{Rice}})$ and is chosen to be $K_R = 3$dB.

Figs. 4 and 5 illustrate the BER performance of the proposed approaches for SIMO and MIMO systems, respectively. In these figures, the performance of the one-tap FEQ is also reported. This FEQ which is similar to the conventional one-tap equalizer, is an extension of the one-tap method in [13] and is derived by minimizing the MSE cost function. From Figs. 4 and 5 it is evident that the one-tap FEQ fails to compensate for the interference. Whereas, the proposed schemes are able to significantly cancel the ICI and IBI. It is also seen that the proposed TEQ and FEQ have almost the same BER performance. Finally, comparing Figs. 4 and 5 shows a diversity gain of about 3.8 dB at BER=10^{-4}.

V. Conclusion

In this paper, time-domain and frequency-domain equalization techniques for UWA MIMO-OFDM systems have been proposed. These equalizers simultaneously combat the rapid time variations and long multipath spread of the UWA channel. The simulation results for a typical underwater channel with Rician fading demonstrate the effectiveness of the proposed techniques.

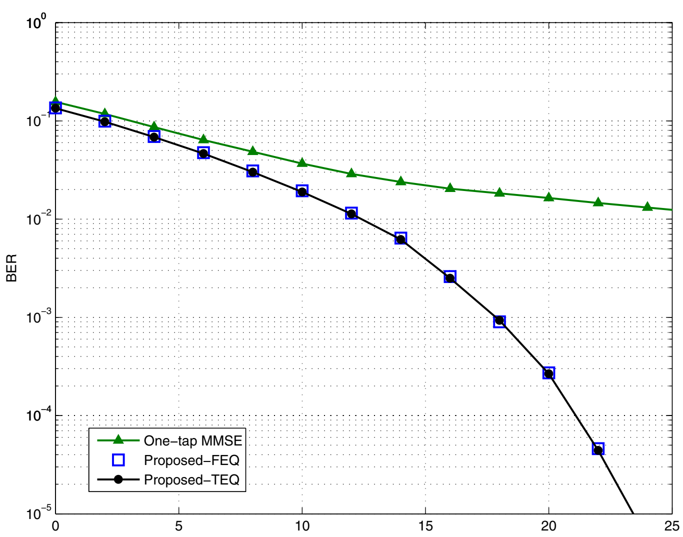

Fig. 4. BER performance for SIMO-OFDM ($N_r = 2$)

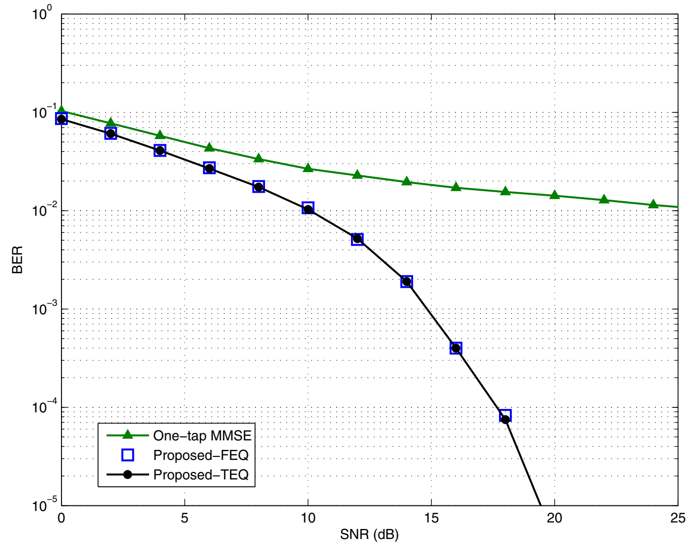

Fig. 5. BER performance for MIMO-OFDM ($N_t = 2, N_r = 4$)

References

[1] J. Tao, Y. R. Zheng, Ch. Xiao, T. C. Yang, and W.-B. Yang, "Channel equalization for single carrier MIMO underwater acoustic communications," *EURASIP J. Advances in Signal Process.*, Article ID 281769, 17 pages, Jan. 2010.

[2] B. Li, J. Huang, S. Zhou, K. Ball, M. Stojanovic, L. Freitag, and P. Willett, "MIMO-OFDM for high rate underwater acoustic communications," *IEEE J. Oceanic Eng.*, vol. 34, no. 4, pp. 634-644, Oct. 2009.

[3] C. R. Berger, Sh. Zhou, J. C. Preisig, and P. Willett, "Sparse channel estimation for multicarrier underwater acoustic communication: from subspace methods to compressed sensing," *IEEE Trans. Signal Process.*, vol. 58, no. 3, pp. 1708-1721, Mar. 2010.

[4] G. Leus and P. Van Walree, "Multiband OFDM for covert acoustic communications," IEEE J. Sel. Areas in Commun., vol. 26, no. 9, pp. 1662-1673, Dec. 2008.

[5] K. Tu, D. Fertonani, T. M. Duman, and P. Hursky, " Mitigation of intercarrier interference in OFDM systems over underwater acoustic channels," in *Proc. of IEEE Oceans Conf.*, Bremen, Germany, May 2009.

[6] Z. Wang, Sh. Zhou, J. Catipovic, and J. Huang, "OFDM in deep water acoustic channels with extremely long delay spread," in *Proc. of ACM Int. Workshop Underwater Netw.*, Massachusetts, USA, Sep. 2010.

[7] J.-Z. Huang, Sh. Zhou, J. Huang, J. Preisig, L. Freitag, and P. Willett, "Progressive MIMO-OFDM reception over time-varying underwater acoustic channels," in *Asilomar Conf. Signals, Systems, and Comp.*, Pacific Grove, CA, Nov. 2010.

[8] M. Beheshti, M. J. Omidi, and A. M. Doost-Hoseini, "Frequency-domain equalization for MIMO-OFDM over doubly selective channels," presented at *Int. Symp. Telecommun.,* Tehran, Iran, Dec. 2010.

[9] G. B. Giannakis and C. Tepedelenlioğlu, "Basis expansion models and diversity techniques for blind identification and equalization of time varying channels," *Proc. IEEE*, vol. 86, no. 10, pp. 1969-1986, Oct. 1998.

[10] A. Stamoulis, S. N., Diggavi, and N. Al-Dhahir, "Intercarrier interference in MIMO-OFDM," *IEEE Trans. Signal Process.*, vol. 50, no. 10, pp. 2451-2464, Oct. 2002.

[11] A. Radosevic, J. Proakis, and M. Stojanovic, "Statistical characterization and capacity of shallow water acoustic channels," in *Proc. IEEE Oceans Conf*, Bremen, Germany, May 2009.

[12] M. J. Omidi, P. G. Gulak, and S. Pasupathy, "Parallel structures for joint channel estimation and data detection over fading channels," *IEEE J. Sel. Areas in Commun.*, vol. 16, no. 9, pp. 1616-1629, Dec. 1998.

[13] Z. Wang and G. B. Giannakis, "Wireless multicarrier communications: where Fourier meets Shannon," *IEEE Signal Process. Mag.*, vol. 17, no. 3, pp. 29-48, May 2000.